Available online at www.sciencedirect.com
ScienceDirect
European Journal of Pharmaceutics and Biopharmaceutics 67 (2007) 309–319
European Journal of Pharmaceutics and Biopharmaceutics
www.elsevier.com/locate/ejpb

Research paper

Solution formulation and lyophilisation of a recombinant fibronectin fragment

P. Pereira [a], S.M. Kelly [b], A. Cooper [c], H.J. Mardon [d], P.R. Gellert [e], C.F. van der Walle [a,*]

[a] *Institute of Pharmacy and Biomedical Sciences, University of Strathclyde, Glasgow, UK*
[b] *Biochemistry and Molecular Biology, University of Glasgow, Glasgow, UK*
[c] *Chemistry Department, University of Glasgow, Glasgow, UK*
[d] *Nuffield Department of Obstetrics and Gynaecology, University of Oxford, Oxford, UK*
[e] *AstraZeneca, Cheshire, UK*

Received 30 October 2006; accepted in revised form 9 March 2007
Available online 19 March 2007

Abstract

The 9th–10th type III fibronectin domain pair shows promise in tissue engineering and tumour vasculature targeting. Calorimetry and structure–function analysis were used to investigate the effects of solution formulation and lyophilisation of a mutant ($^{9-10}$FNIII-P). A single endothermic transition for $^{9-10}$FNIII-P in solution was observed at pH < 8, irrespective of addition of sucrose or PEG. The temperature at the maximum heat capacity (T_m) and enthalpy (ΔH) of the transition increased for increasing sucrose concentrations but decreased for increasing PEG concentrations. The transition was fitted to a single two-state unfolding mechanism (in contrast to unfolding in guanidine·HCl) and was partially reversible only at pH 4, with increasing concentrations of sucrose causing a marked fall in ΔH between scans. Circular dichroism spectra for the thermal unfolding of $^{9-10}$FNIII-P at pH 4 showed loss of native β-sheet structure and loss of aromatic contributions to the peak centred around 226 nm yielding an intermediate conformation, which in the presence of sucrose was more disordered. Despite a glass transition (T'_g) for $^{9-10}$FNIII-P$_{(aq)}$ of −70 °C, primary drying at −30 °C did not perturb its conformation upon reconstitution or its biological activity following lyophilisation; the addition of sucrose or PEG had no influence on structure or activity. The main consideration in the formulation of $^{9-10}$FNIII-P was therefore pH.

Keywords: Fibronectin; Thermal stability; Calorimetry; Circular dichroism; Cell adhesion; Formulation

1. Introduction

The recombinant central cell binding domain of fibronectin ($^{9-10}$FNIII) promotes cell attachment and spreading on binding to α5β1-integrin receptors: the 9th type III FN domain harbouring the 'synergy site' which, together with the Arg-Gly-Asp (RGD) site on the 10th type III FN domain, is required for full binding affinity [1]. Since α5β1-integrin mediates osteoblast differentiation, angiogenesis, tumorigenesis and embryo implantation, $^{9-10}$FNIII has good potential for use in tissue engineering, anti-cancer and implantation therapies [2–4]. Surprisingly, little is known about the solution conditions that stabilise $^{9-10}$FNIII or other 3 + 4 β-sandwich FNIII-type domains. Establishing such conditions would be the first step to identifying parameters suitable for formulation development of $^{9-10}$FNIII, in order to achieve an acceptable shelf life and maintain biological activity.

Here, we evaluate the effect of solution pH and additives on the structural stability of $^{9-10}$FNIII in the liquid and solid states. Specifically, the protein used is a mutant of the 9th–10th FN type III domains (termed $^{9-10}$FNIII-P), wherein Leu^{1408} is substituted for Pro, which increases conformational stability and biological activity [5]. The calculated isoelectric point, pI, for $^{9-10}$FNIII-P is 8.1 and, in

* Corresponding author. Institute of Pharmacy and Biomedical Sciences, University of Strathclyde, 27 Taylor Street, Glasgow, UK. Tel.: +44 (0) 141 548 5755; fax: +44 (0) 141 552 2562.
E-mail address: chris.walle@strath.ac.uk (C.F. van der Walle).

0939-6411/$ - see front matter © 2007 Elsevier B.V. All rights reserved.
doi:10.1016/j.ejpb.2007.03.009

order to establish the optimum solution pH, experiments were performed for pH intervals from 4 to 8. The additives used were sucrose and polyethylene glycol (PEG), chosen as representatives of commonly used protein lyoprotectants and cryoprotectants. Lyo- and cryo-protection afforded by sucrose is thought to occur through its preferential exclusion from the protein/polypeptide surface [6], thermodynamically favouring the folded state [7], or via hydrogen bonding with polar groups on the protein surface [8]. The level of stabilization afforded by sugars is usually dependent on their bulk concentration. In contrast, the stabilisation mechanism of PEG on proteins is less well established and may occur through steric hindrance of protein–protein interactions, increased solution viscosity and decreased protein structural mobility [9].

The thermal stability of $^{9-10}$FNIII-P in the liquid state was studied using differential scanning calorimetry (DSC) to assess the behaviour of proteins over a wide range of temperatures [10]. DSC is a commonly utilised technique to study the effect of formulation variables on protein stability, using simple heat–cool cycles to evaluate thermal reversibility of protein unfolding [11,12]. For simple 2-state equilibrium unfolding, the maximum point on the heat capacity curve (T_m, the "melting temperature") is the temperature at which 50% of the protein molecules are unfolded. Although 2-state equilibrium criteria rarely apply for proteins under physiological conditions, T_m remains a useful indicator of protein stability between different formulations as a measure of the apparent stability to thermal unfolding and other degradation processes in solution. It should be noted that T_m can be lowered by excipients such as PEG, although a stabilization is achieved at room temperature. The DSC data were supported by analysis of the secondary structure of the protein using circular dichroism (CD) and environment of the Trp residues via their intrinsic fluorescence [13], for the same formulation variables and increase in temperature. The structure of $^{9-10}$FNIII is known from X-ray diffraction and NMR studies [14,15] (Fig. 1 shows the $^{9-10}$FNIII-P domain pair) and there have been a number of studies which have characterised the wild type FNIII by circular dichroism (CD) [16,17]. The latter have shown that aromatic residues also contribute to the far UV CD spectrum, particularly with respect to the positive peak centred around 226 nm. The differences in spectra obtained for each formulation approach were interpreted to reflect changes in the environment of aromatic residues and/or changes in the β-sandwich fold of the protein.

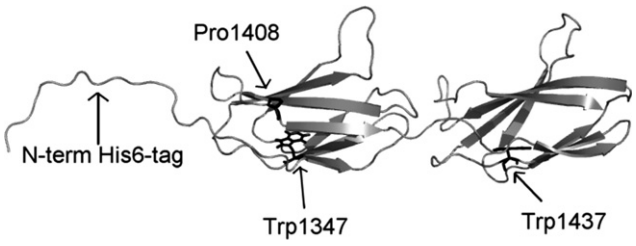

Fig. 1. Ribbon diagram of the three-dimensional structure of the histidine-tagged $^{9-10}$FNIII-P recombinant protein. β Strands are shown as grey ribbons. Amino acid substitutions that were used in the study are shown in black with side chains as stick diagrams.

Lyophilisation is often chosen to stabilise proteins as a way to minimize chemical and physical instabilities [18]. The same formulations used for the liquid state studies were again used to investigate the effect of lyophilisation of $^{9-10}$FNIII-P on its structure and function. The design of a lyophilisation cycle requires that several parameters be taken into account to bring to a minimum the freezing and drying stresses on the protein and to have a reproducible and feasible cycle. Some of the most important parameters to be determined prior to the establishment of a lyophilisation cycle are the glass transition temperatures, or T'_g, of the protein and the excipients (e.g. sucrose) in solution [19]. The T'_g of a protein in solution is analogous to the T_g of an amorphous polymer; below this temperature the protein molecules exist in a glassy state with no long-range molecular mobility [20]. At temperatures above the T'_g the protein gains molecular mobility, albeit that unfolding is much slower than the time for lyophilisation. Nevertheless, some proteins can be lyophilised well above T'_g without undergoing detrimental denaturation [21]. Here, we relate the T'_g of $^{9-10}$FNIII-P to the lyophilisation cycle employed. In order to determine the influence of the formulation conditions and lyophilisation process on the biological activity of $^{9-10}$FNIII-P, cell adhesion assays were performed. Lyophilised protein samples were also reconstituted with water to investigate changes to the $^{9-10}$FNIII-P structure by CD.

2. Materials and methods

2.1. Materials

Potassium chloride, sodium chloride, sodium acetate, polyethylene glycol Mw 6000 (PEG 6000), sucrose and polyvinyl alcohol were purchased from Sigma Chemical Company, Dorset, UK, at analytical quality. Sodium and potassium dihydrogen orthophosphate and di-sodium hydrogen orthophosphate were supplied by Fisher Scientific, Leicestershire, UK.

2.2. Expression and purification of $^{9-10}$FNIII-P

$^{9-10}$FNIII-P (MW 21468) was expressed in *Escherichia coli* BL21 (DE3) pLysS extended at the N-terminus by a polyhistidine tag to facilitate purification by metal chelation chromatography, as previously described [5]. Briefly, *E. coli* were transformed with the pRSETa-$^{9-10}$FNIII-P construct and grown in LB to OD_{600} 0.6, when 0.1 mM of isopropyl-β-D-thiogalactopyranoside was added to induce expression; cells were harvested 3 h later, lysed and the supernatant clarified. Eluted protein fractions from a Ni^{2+}–Sepharose column were concentrated and further

purified by gel chromatography (300 ml Superdex 75 prep grade resin, Amersham Biosciences, UK), equilibrated with phosphate-buffered saline (PBS: 137 mM NaCl, 2.7 mM KCl, 10 mM Na_2HPO_4, 2 mM KH_2PO_4, pH 7.4). Purity was assessed by sodium dodecyl sulphate–polyacrylamide gel electrophoresis (SDS–PAGE) and concentrations were calculated using the A_{280} value and a calculated extinction coefficient (ε) of 21,620 M^{-1} cm^{-1}. Proteins were concentrated to 1 mg/ml and stored at −80 °C.

2.3. Differential scanning calorimetry (DSC)

Solution DSC experiments measuring the thermal unfolding of $^{9-10}$FNIII-P were made using a MicroCal VP-DSC calorimeter. Protein concentrations were kept between 0.05 ± 0.012 mM at pH 4 (10 mM CH_3COONa), pH 7 and pH 8 (10 mM NaCl, 50 mM NaH_2PO_4). The choice of acetate/phosphate buffers is a consequence of the pH required, the addition of NaCl at pH 7 is based on previous emulsion-stability studies with $^{9-10}$FNIII [22]. Sucrose was added at concentrations of 0.05, 0.28 and 0.5 M, and PEG 6000 at 1, 3 and 5% (w/v). Prior to each experiment, samples were thoroughly dialysed overnight against the corresponding buffers and degassed briefly under vacuum before loading. Consecutive scans (to a maximum of five) were performed over a temperature range of 20–80 °C at a scan rate of 60 °C/h. Buffer baselines were obtained and subtracted from the sample data before analysis with Microcal Origin 5.0™ software.

The glass transition (T'_g) for $^{9-10}$FNIII-P was determined with a Mettler Toledo DSC822e calorimeter. An aluminium pan was loaded with 25 μl of the protein solution (20 mg/ml, equivalent to 0.5 mg protein); PBS was used as the reference in a weight-matched aluminium pan. Samples were initially cooled from 25 to −50 °C at a cooling rate of 10 °C/min and then from −50 to −80 °C with a 2 °C/min cooling rate. Following an isothermal step at −80 °C for 5 min, samples were heated to 25 °C with a 2 °C/min heating rate. Measurements were performed in duplicate.

2.4. Lyophilisation

Lyophilisation was performed using an Advantage freeze dryer (Virtis). One millilitre of a 1 mg/ml (ca. 0.05 mM) solution of $^{9-10}$FNIII-P was lyophilised; solutions were buffered appropriate to the pH and with and without additives (Section 2.3). Shelf and mock sample (1 ml PBS) temperatures and vacuum were recorded throughout. The shelf temperature of the freeze-drier was brought to 5 °C and held for 30 min. Samples were further cooled to −5 °C and kept at this temperature for 30 min before cooling to −30 °C at a rate of 1 °C/min, and maintained for 1 h. Primary drying was initiated at −30 °C over 1000 min, with a chamber pressure of 100 mTorr. The chamber was then heated to 25 °C at a 0.1 °C/min and samples dried for a further 3 h, before final equilibration of pressure and temperature. Lyophilised samples reconstituted with 400 μl of distilled water immediately before analysis.

2.5. Circular dichroism (CD)

CD spectra were recorded for $^{9-10}$FNIII-P at a concentration of 0.05 mM in 10 mM sodium acetate buffer, pH 4, in the absence and presence of 0.5 M sucrose, using a Jasco 810 spectropolarimeter. Spectra were recorded in the far UV region (187–260 nm), using a 0.02 cm pathlength cell, with a 50 nm/min scan speed, a 0.5 s time constant, 1 nm bandwidth and accumulation of 8 scans in each case. Temperature measurements were recorded at 5 °C increments from 4 to 79 °C using a Peltier device. The protein was incubated for 3 min at each temperature before a spectrum was recorded. For the second cycle the temperature was lowered to 4 °C and allowed to equilibrate for 20 min before starting the measurements.

CD spectra for reconstituted lyophilised samples were recorded for $^{9-10}$FNIII-P lyophilised from solution at pH 4 without additives and with 0.5 M sucrose and 1% PEG 6000. CD spectra recorded as above in the far UV and the near UV regions (260–180 nm and 320–250 nm, respectively) using a bandwidth of 1 nm, a scanning rate of 50 nm/min, a response time of 0.5 s and a data pitch of 0.2 nm. The T_m of the protein obtained by CD was taken as the inflection point of a plot of the percentage total change at 226 nm (corresponding to the aromatic residues) versus temperature.

2.6. Fluorescence spectroscopy

Fluorescence spectra were recorded using a Varian Cary Eclipse spectrofluorimeter, equipped with a Peltier controlled thermostatted cell holder, with λ_{ex} 295 nm and λ_{em} 300–450 nm. $^{9-10}$FNIII-P samples were kept at 0.012 ± 0.001 mM with buffers and additives as described in Section 2.3. The temperature was increased from 20 to 80 °C in 10 °C increments. A customized pressure device was built to maintain the samples at 25 psi, equivalent to the pressure applied during the thermal unfolding experiments (Section 2.3). Protein aggregation was monitored by turbidity measurements at 320 nm for the protein solution in quartz semi-micro cuvettes of pathlength 1 cm (Hellma, Germany), using a Unicam UV-300 spectrometer.

2.7. Inhibition of cell spreading assay

Spreading of Baby Hamster Kidney (BHK) cells on surfaces requires natively folded $^{9-10}$FNIII [23] and was measured in preference to simple cell adhesion, which is not dependent on natively folded protein [24]. Lyophilised protein samples were reconstituted in distilled water. Tissue culture plates were coated with fibronectin (10 μg/ml) overnight and washed the next day 3× in PBS. Wells were then blocked by addition of 1% BSA in PBS for 1 h and washed

again in PBS. Confluent BHK cells were trypsinised from the surface, subsequently using trypsin inhibitor rather than serum to prevent interference in the adhesion assay. To each well in a pair, 50 μl of BHK cells (10^4 cells) was added and gently mixed with $^{9–10}$FNIII-P over various concentrations. The plate was incubated at 37 °C for 1 h and non-adherent cells gently washed off in PBS. Cells were fixed with formaldehyde for 20 min and spread cells versus non-spread cells were scored as described previously [1].

Experiments were repeated in quadruplicate to obtain data as means ± SEM. Statistical analysis of the inhibition of cell adhesion for increasing concentrations of $^{9–10}$FNIII-P samples was performed using a one way analysis of variance with Dunnett's post test (comparing groups against the non-lyophilised $^{9–10}$FNIII-P control). A significance level of $P < 0.05$ was used to denote significance in all cases. All analyses were performed using GraphPad Prism ver. 4.1, GraphPad Software, CA, USA.

3. Results and discussion

3.1. Calorimetric analysis of the thermal transition of $^{9–10}$FNIII-P

DSC thermograms obtained for $^{9–10}$FNIII-P in pH 4 buffered solution all showed a single sharp endothermic transition (Fig. 2a); in the absence of additives the maximum point on the heat capacity curve, T_m, occurred at 59.7 °C (Table 1). Repeated temperature scans showed a marked decrease in the enthalpy (ΔH, the area under the curve) for the protein transition, particularly between the first and second cycles. The single endothermic transition, reflecting the disruption of the native $^{9–10}$FNIII-P structure, was indicative of a single two-state unfolding transition. After normalisation of the data for protein concentration and baseline correction, the data were fitted to several models, following the Levenberg–Marquardt non-linear least-square method. In pH 4 buffered solution, the model of best fit to the data was one assuming a dynamic, reversible two state equilibrium. With the fitted data, analysis of the mechanism of unfolding was further performed by comparing the enthalpy ΔH with the van't Hoff enthalpy ΔH_v (determined from the shape of the thermogram). The $\Delta H/\Delta H_v$ ratio was calculated as 0.75 suggesting that the 9th and 10th type III domains unfolded co-operatively (being close to a ratio of 1.0), rather than unfolding independently (which would yield a ratio of 2.0). Deviation from a ratio of 1.0 was most likely due to the error in the fit of the theoretical curve against the experimental data, particularly where somewhat noisy baselines were observed either side of the transition, compromising the statistical fitting approach. The observation of co-operative unfolding for the domain pair is interesting since unfolding of $^{9–10}$FNIII in increasing concentrations of guanidine.HCl (GuHCl) has been shown by NMR and fluorescence data to occur via a two-step process, wherein the more unstable ^{9}FNIII domain unfolds completely before unfolding of the ^{10}FNIII domain [25]. The same two-step transition is observed for GuHCl-denaturation of $^{9–10}$FNIII-P [5], although unfolding of $^{9–10}$FNIII and

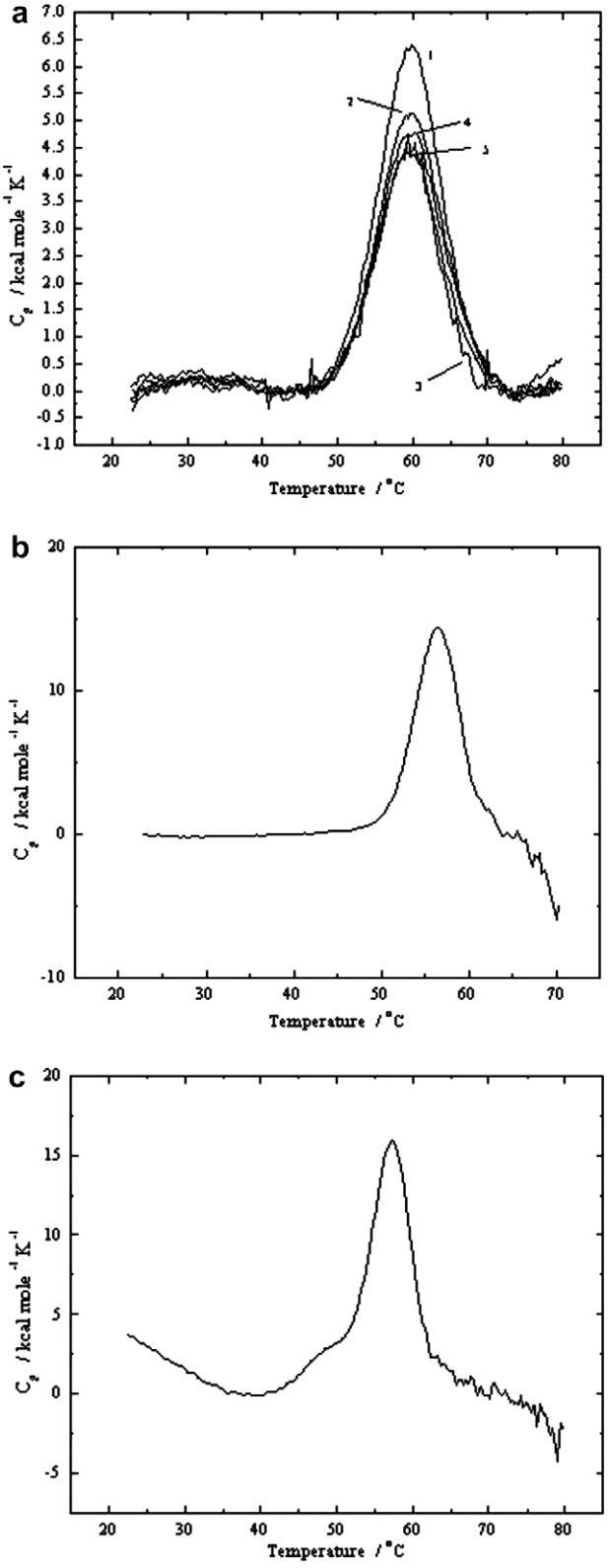

Fig. 2. Heat capacity curves showing the thermal transition of $^{9–10}$FNIII-P over five repeated heat–cool cycles (corresponding to numbers assigned to each curve) in buffered solution at pH 4 (a), pH 7 (b) and pH 8 (c).

Table 1
Solution DSC data for $^{9-10}$FNIII-P and curve fitting

	T_m 1st cycle (°C)	ΔH 1st cycle (kcal/mol, χ^2 fitting parameter)	ΔH_v 1st cycle (kcal/mol)	$\Delta H/\Delta H_v$ 1st cycle	T_m 2nd cycle (°C)	ΔH 2nd cycle (kcal/mol, χ^2 fitting parameter)	ΔH_v 2nd cycle (kcal/mol)	$\Delta H/\Delta H_v$ 2nd cycle
pH 4 no additive	59.69	6.46×10^4 (5.59×10^4)	8.54×10^4	0.76	59.59	5.05×10^4 (5.68×10^4)	8.57×10^4	0.59
pH 7 no additive	56.37	9.49×10^4 (3.96×10^7)*	1.33×10^5	0.71	n/a			
pH 8 no additive	T_m peak 1: 49.19	ΔH peak 1: 2.18×10^4	ΔH_v peak 1: 9.48×10^4	0.23	n/a			
	T_m peak 2: 57.2	ΔH peak 2: 1.08×10^5 (1.51×10^6)*	ΔH_v peak 2: 1.25×10^5	0.86				
pH 4 0.05 M sucrose	59.30	5.87×10^4 (1.51×10^4)	9.25×10^4	0.63	59.26	3.7×10^4 (8.13×10^3)	8.88×10^4	0.42
pH 4 0.28 M sucrose	61.07	6.33×10^4 (4.62×10^5)	9.91×10^4	0.64	60.98	3.51×10^4 (2.22×10^4)	9.6×10^4	0.37
pH 4 0.5 M sucrose	62.41	6.46×10^4 (7.07×10^5)	1.0×10^5	0.65	62.35	3.61×10^4 (1.22×10^4)	9.83×10^4	0.37
pH 4 1% PEG 6000	59.02	6.66×10^4 (9.33×10^4)	8.42×10^4	0.79	59.05	5.79×10^4 (1.64×10^4)	8.11×10^4	0.71
pH 4 3% PEG 6000	58.43	7.23×10^4 (1.45×10^5)	8.16×10^4	0.89	58.52	4.72×10^4 (1.00×10^4)	8.58×10^4	0.55
pH 4 5% PEG 6000	58.35	4.85×10^4 (7.37×10^4)	1.0×10^5	0.49	58.32	3.36×10^4 (2.46×10^4)	9.2×10^4	0.37

Data acquired at pH 8 were best fitted to a two-step unfolding process; *, these thermograms had noisy baselines above 60 °C, which was the probable cause for the poor fit of the theoretical curves to the experimental data, giving high χ^2 values; n/a, precipitation of the protein prevented a second heat cycle being performed.

mutants thereof in sodium dodecyl sulphate is co-operative [22].

For $^{9-10}$FNIII-P in pH 7 buffered solution, a single endothermic transition was noted but with a noisy baseline above 60 °C, indicative of protein precipitation (Fig. 2b); on subsequent heat cycles no transition was observed. In pH 8 buffered solution, thermograms for $^{9-10}$FNIII-P showed a shoulder leading into the main peak in addition to a noisy baseline above 60 °C, with no transition observed on repeated heat cycles (Fig. 2c). The thermograms acquired at pH 8 were best fitted to a two-step thermal unfolding model, though the fit between theoretical and experimental data was poor (Table 1). It could not be determined whether domain pair unfolding was independent above pH 7 or whether subpopulations of $^{9-10}$FNIII-P conformers existed. However, protein refolding was clearly completely irreversible at pH 7 and 8, which are around the calculated pI of 8.1 for $^{9-10}$FNIII-P. Thus, pH values around the pK_a of the acidic amino acid side chains (i.e. far below the pK_a values of histidine, arginine and lysine side chains) appeared to be critical to the stabilisation of $^{9-10}$FNIII-P in solution. It is worth noting that $^{9-10}$FNIII-P has more basic amino acids (28) than acidic (17), although the overall charge at a certain pH cannot be calculated theoretically (treating the residues as isolated) since this depends on the protein conformation. A possible reason for the increased stability of the protein may therefore relate to the complete ionisation of the basic groups, including the polyhistidine tag.

For the protein in pH 4 buffered solution containing sucrose, the same single endothermic transition was also observed (Fig. 3a–c). Increasing the concentration of sucrose resulted in an increase in the T_m to 62.4 °C at 0.5 M sucrose, with corresponding increases in ΔH (Table 1). This increase in unfolding enthalpy with temperature is typical of the positive heat capacity increment (ΔC_p) commonly seen for proteins in solution [10]. Using T_m in this comparative manner therefore suggested that increasing sucrose concentrations to 0.5 M increased $^{9-10}$FNIII-P stability, consistent with previous data for other proteins [6,11,12]. The ΔH between the first and second heat cycles was markedly decreased on addition of sucrose (Table 1); the fall in ΔH between subsequent heat cycles being negligible. This observed difference in the fall in ΔH between heat cycles indicated a change in the refolding of $^{9-10}$FNIII-P, resulting in an intermediate structure with a lower ΔH during reheating. Non-specific polypeptide aggregation seemed unlikely since no precipitate was observed at this pH. However, it was clear that heat-denatured $^{9-10}$FNIII-P did not refold to its native structure, and that the fraction of non-natively folded protein increased on addition of sucrose. It is worth noting that the rate of refolding of GuHCl-denatured ^{10}FNIII occurs orders of magnitude more rapidly than ^{9}FNIII refolding [26]. Thus, there existed the possibility that following the first heat cycle, ^{9}FNIII was irreversibly unfolded whereas ^{10}FNIII returned to its native state. Further structural data using

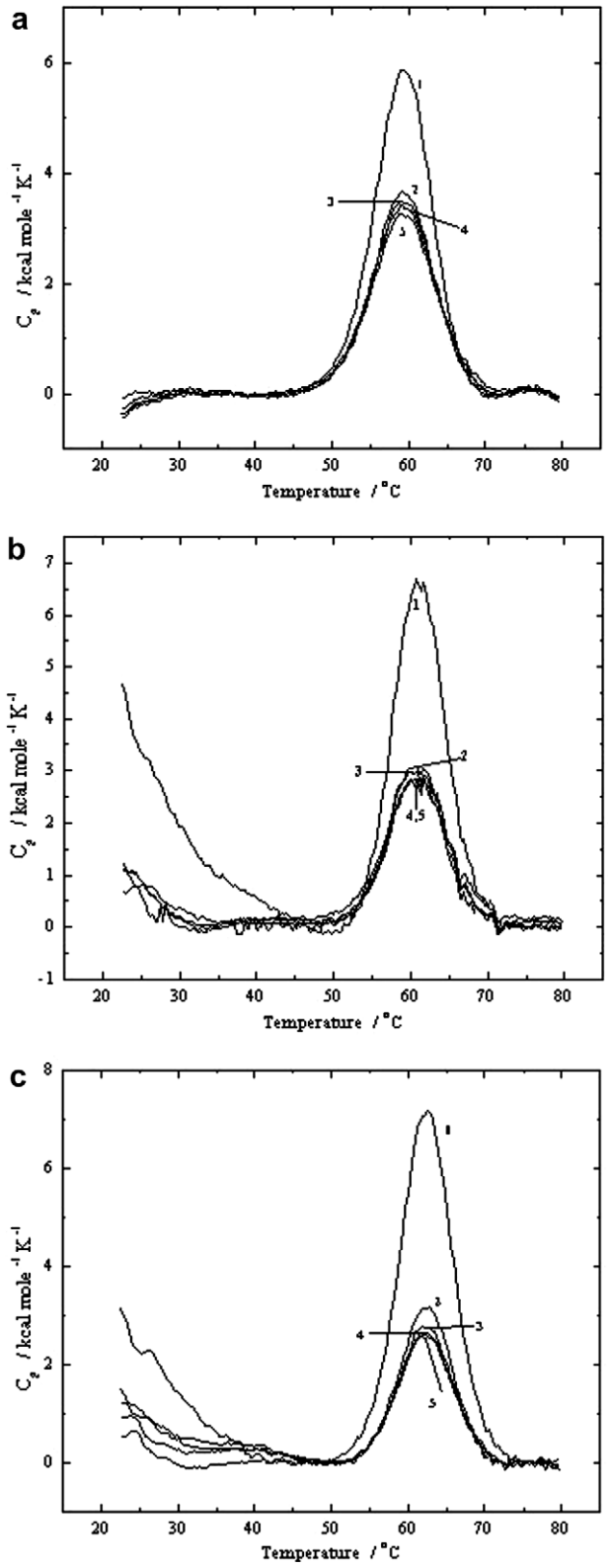

Fig. 3. Heat capacity curves showing the thermal transition of $^{9-10}$FNIII-P over 5 repeated heat–cool cycles (corresponding to numbers assigned to each curve) in pH 4 buffered solution containing 0.05 M sucrose (a), 0.28 M sucrose (b) and 0.5 M sucrose (c).

CD and fluorescence were therefore acquired to clarify the unfolding of $^{9-10}$FNIII-P during heat–cool cycles and the effect of sucrose.

For the addition of PEG 6000 to $^{9-10}$FNIII-P, pH 4, the single endothermic transition remained but with T_m values decreasing to 58.4 °C at 5% PEG 6000 (Fig. 4a–c and Table 1). Accordingly, PEG 6000 had a small destabilising effect on $^{9-10}$FNIII-P in pH 4 buffered solution. However, in contrast to sucrose, smaller, stepwise falls in ΔH between heat cycles were observed, suggesting some maintenance in unfolding reversibility. The interaction of PEGs with protein can be complex, including stabilisation of unfolded or intermediate states [27]. If stabilisation of the non-native state shifts the folded–unfolded equilibrium to the right (towards the final state as described in the Lumry–Eyring model [28]) then this interpretation would be consistent with the observed fall in the T_m and may explain the apparent preservation of unfolding reversibility of $^{9-10}$FNIII-P, compared to that afforded by sucrose. It is noteworthy that the fall in ΔH between repeated heat cool cycles was not progressive: under all conditions tested, the largest fall in ΔH was observed between the first and second heat cycles. Smaller falls in ΔH were observed thereafter, with, particularly, little or no change observed when sucrose was added to the solution. An explanation to account for this cannot be provided without further investigations possibly involving amino acid substitutions probing possible *trans* to *cis* proline isomerization.

3.2. Structural analysis of the thermal denaturation of $^{9-10}$FNIII-P

The CD spectrum for $^{9-10}$FNIII-P in pH 4 buffered solution (Fig. 5) gave a shape characteristic of a predominantly β-sheet/turn protein which is consistent with the known structure [14,15]; overall the shape was similar to the previously reported spectrum of wild type fibronectin [17] with a positive CD band centred around 226 nm, a weaker negative maximum centred around 215 nm and a stronger positive maximum centred around 202 nm. Stepwise increments in temperature between 4 and 40 °C did not markedly reduce the maximum ellipticity at 226 nm or shift its position (a decrease in ellipticity of around 10% was observed, Fig. 6a and c). Above 45 °C a progressive decrease in the ellipticity values centred around 226 nm was observed probably reflecting a change in both secondary and tertiary structure of the protein. The temperature corresponding to a structural transition in $^{9-10}$FNIII-P is coincident with the endothermic transition observed by DSC measurements. The apparent T_m value as judged by CD spectra occurred around 55 °C. The spectra obtained at temperatures above 54 °C were not characteristic of random coil suggesting that residual secondary structural elements remained. Given that the aromatic residues are believed to contribute to the peak centred around 226 nm it is likely that as the protein is heated these residues are placed in a less rigid environment which would diminish their contributions in this region. Subsequent cooling showed only β-sheet structure, i.e. there was no recovery in the peak centred around 226 nm and therefore no evi-

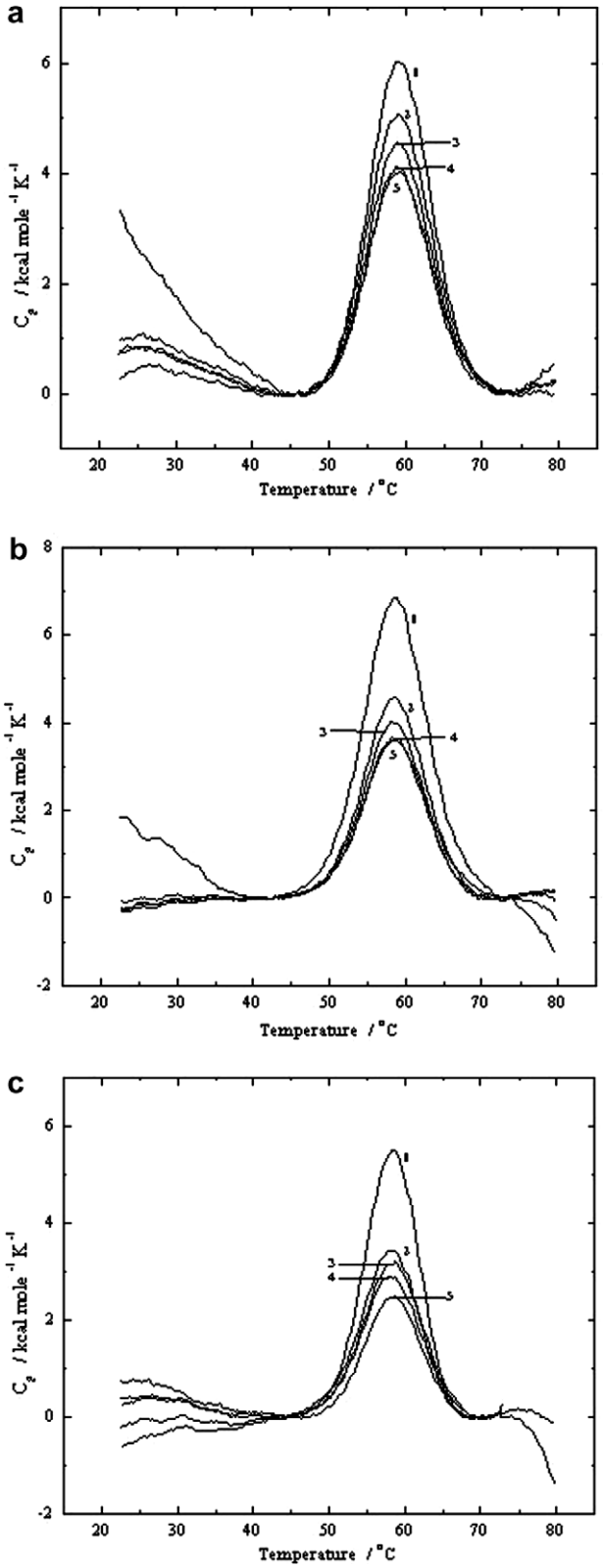

Fig. 4. Heat capacity curves showing the thermal transition of $^{9-10}$FNIII-P over five repeated heat–cool cycles (corresponding to numbers assigned to each curve) in pH 4 buffered solution containing 1% w/v PEG 6000 (a), 3% w/v PEG 6000 (b) and 5% w/v PEG 6000 (c).

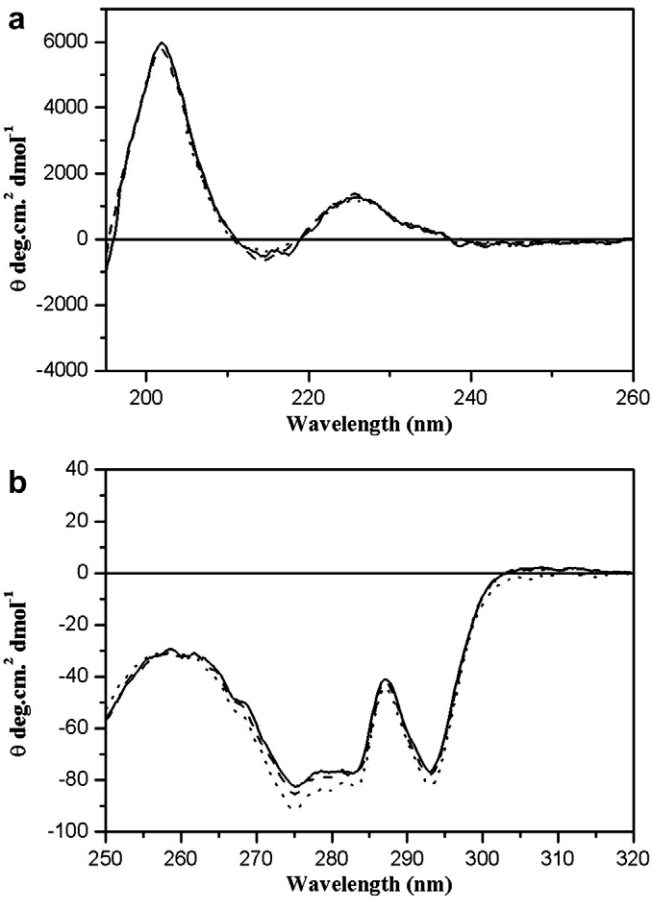

Fig. 5. Far (a) and near (b) UV CD spectra of $^{9-10}$FNIII-P in pH 4 buffered solution (solid), containing 0.5 M sucrose (dotted) and 1% PEG 6000 (dashed).

dence of refolding of $^{9-10}$FNIII-P to its native structure. The intermediate formed following the first thermal cycle was found to be stable in that no further changes in the CD spectra were observed during the 2nd thermal cycle.

Fluorescence analysis of $^{9-10}$FNIII-P unfolding in pH 4 buffered solution showed a red shift in the maximum emission peak (from around 315 to 335 nm) during heating between 50 and 60 °C (Fig. 7a), suggesting the local Trp environment became more polar, consistent with unfolding of the structure as seen by CD. An increase in fluorescence intensity was concomitant with the red shift of the maximum emission, which is somewhat unusual but has previously been noted for GuHCl unfolding of $^{9-10}$FNIII and $^{9-10}$FNIII-P [5,25]. Turbidity measurements for the protein in pH 4 buffered solution did not show evidence of protein aggregation by during the heat–cool cycle, consistent with the (partial) refolding reversibility observed during DSC analysis at pH 4. Repeating the experiment at pH 7 and 8 gave the same red shift in the peak emission maximum above 50 °C but precipitation of the sample quickly followed (preventing further accurate measurement); this being consistent with the DSC data showing non-reversible protein unfolding and aggregation above pH 4.

Interpreting the DSC data in the light of the CD and fluorescence data suggested that the fall in ΔH between heat cycles for $^{9-10}$FNIII-P at pH 4 was due to a non-natively folded intermediate, rather than a mixed population of unfolded/folded ^{9}FNIII/^{10}FNIII domains. The stability of the $^{9-10}$FNIII-P β-sheet intermediate appears to be dependent upon mildly acidic conditions since both fluorescence and DSC data show that irreversible protein denaturation occurred at pH 7 and 8.

3.3. The effect of additives on the structural stability of $^{9-10}$FNIII-P

Due to the strong far UV absorption of sucrose, the CD spectrum of FNIII in the presence of this osmolyte was truncated at 205 nm. Addition of sucrose or PEG 6000 to $^{9-10}$FNIII-P in pH 4 buffered solution did not significantly alter the β-turn structure of the protein in the far UV regions (Fig. 5a), with only small changes in the near UV region observed for the addition of sucrose (Fig. 5b). For $^{9-10}$FNIII-P in pH 4 buffer containing 0.5 M sucrose the structure was found to be slightly more stable with an apparent T_m of 63 °C (Fig. 6b and c), i.e. higher than for $^{9-10}$FNIII-P in pH 4 buffer alone which is consistent with the increase in T_m observed by DSC. The spectra obtained as the temperature was raised above 44 °C did not mirror the spectral shapes observed during the unfolding of $^{9-10}$FNIII-P in the absence of sucrose, suggesting that the presence of this osmolyte altered the unfolding pathway in some way. At 79 °C the spectrum appeared to be more disordered than that for $^{9-10}$FNIII-P at 79 °C in pH 4 buffer alone. On cooling, the shapes of the CD spectra of the osmolyte-containing protein and protein in buffer alone were different (Fig. 6b vs. a). Therefore, although the presence of sucrose appears to stabilise $^{9-10}$FNIII-P during heating it is possible that this is by way of adopting an alternative unfolding pathway which proceeds to a less ordered state. It is possible that the unfolding pathway

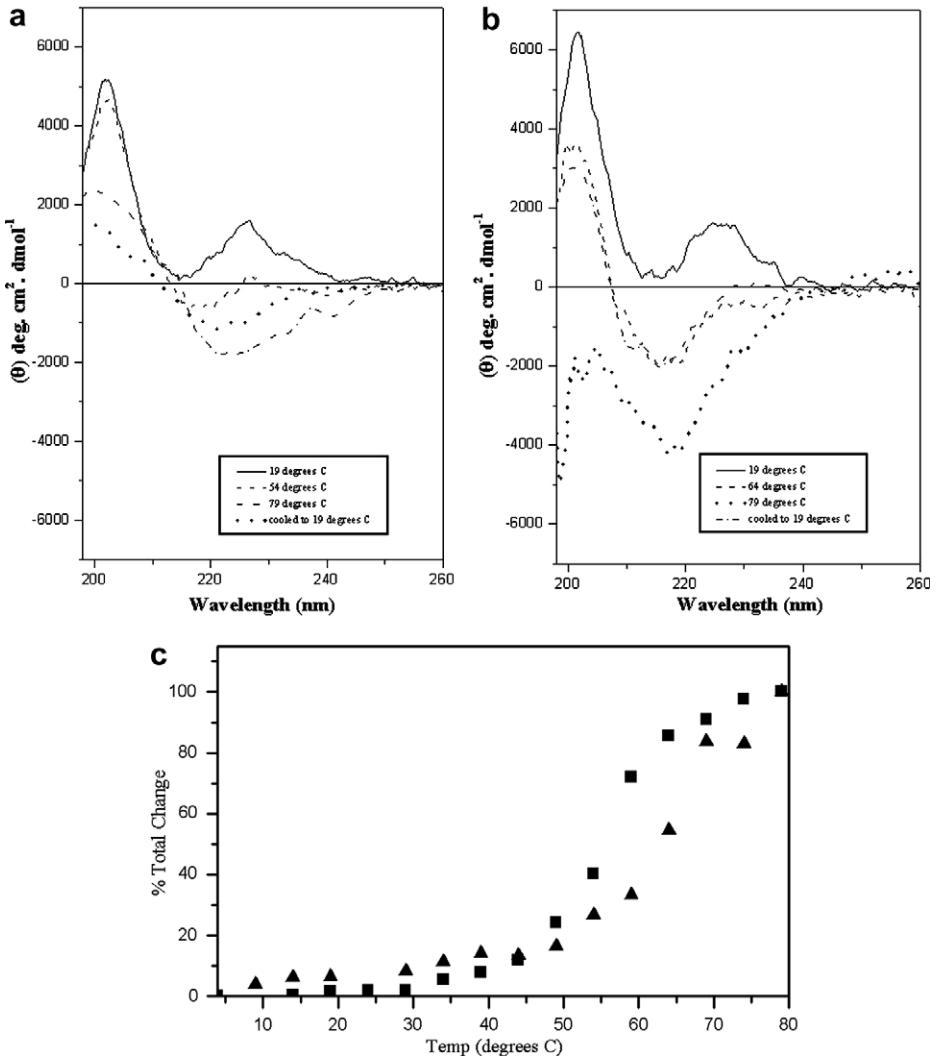

Fig. 6. Far UV CD spectra of $^{9-10}$FNIII-P in pH 4 buffered solution following thermal unfolding in the absence (plot a and plot c: squares) and presence (plot b and plot c: triangles) of 0.5 M sucrose.

adopted by the protein in buffer alone results in the formation of a more stable intermediate which requires higher temperatures (>70 °C) to denature further. It is interesting to note that heating the protein to 79 °C in buffer alone appeared to result in an irreversibly 'trapped' intermediate, in that no change was observed upon cooling and re-heating. The protein formulated in sucrose regained some of its structure upon cooling, adopting a structure similar to that observed at 64 °C.

By fluorescence analysis, the addition of sucrose or PEG 6000 to $^{9-10}$FNIII-P in pH 4 buffered solution did not shift the emission peak maximum (Fig. 7b and c). However, the emission intensity decreased for addition of sucrose, indicating a small shift in the Trp environment consistent with the small changes observed in the near UV CD spectrum in the presence of sucrose (Fig. 5b). Trp fluorescence monitored during heating of $^{9-10}$FNIII-P in the presence of sucrose and PEG 6000 showed a red shift in the peak maxima above 50 °C accompanied by an increase in intensity. These profiles were similar to that seen for $^{9-10}$FNIII-P in pH 4 buffered solution alone, indicating that the Trp environment became more polar during heating, consistent with the observed protein unfolding monitored by CD.

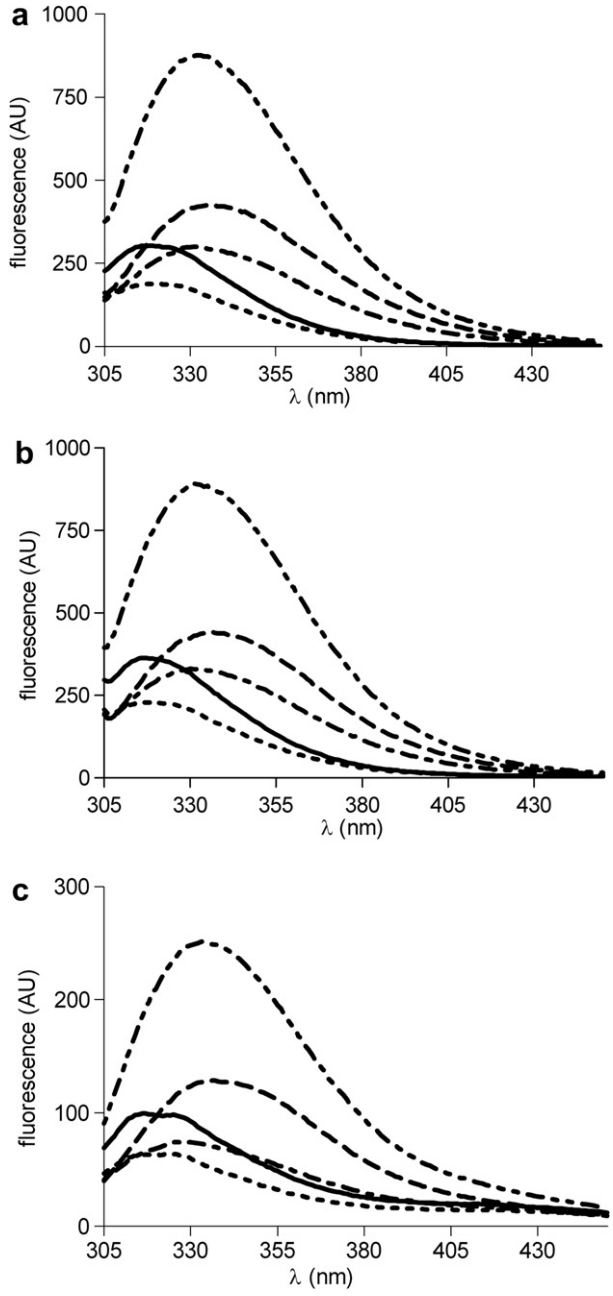

Fig. 7. Fluorescence emission spectra for $^{9-10}$FNIII-P (λ_{ex} 295 nm), 0.012 mM, pH 4 (a), pH 7 (b) and pH 8 (c). Selected spectra acquired at 20 °C (solid line), 50 °C (dotted line), 60 °C (dot-dashed line), 80 °C (dashed line) and cooling back to 20 °C (dot-dot-dashed line) are shown.

3.4. Lyophilisation of $^{9-10}$FNIII-P and structure–function analysis

Calorimetric analysis for $^{9-10}$FNIII-P frozen in solution during heating from −80 °C showed a clear endothermic shift in specific heat capacity and a discontinuity in the baseline (Fig. 8). This represents a typical glass transition, the mid-point of the transition (T'_g) occurring at −70.1 °C, which is in accordance with the values found for other proteins in solution [29]. The same scan for buffer alone showed that the endothermic shift was not due to the presence of salt in the buffer (Fig. 8, inset) [30]. Aiming for a primary drying cycle at temperatures below the T'_g was therefore unrealistic, and lyophilisation of $^{9-10}$FNIII-P was conducted at more typical temperatures, well above its T'_g. Evidence for absence of irreversible protein denaturation was obtained by reconstitution of the solid samples and structure–function analysis. Far UV CD spectra for samples reconstituted from 0.5 M sucrose and 0.1% PEG 6000 matched entirely CD spectra for non-lyophilised samples under the same conditions (data not shown), demonstrating that the overall β-turn structure of $^{9-10}$FNIII-P was maintained regardless of lyophilisation in the presence of sucrose or PEG 6000. Therefore, primary drying at temperatures well above the T'_g of $^{9-10}$FNIII-P was not detrimental to the structural integrity of $^{9-10}$FNIII-P.

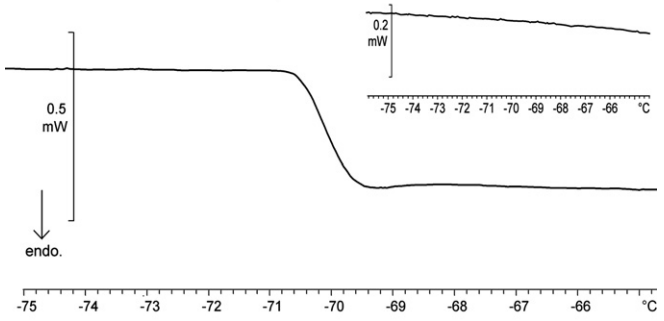

Fig. 8. Total heat flow DSC heating thermograms normalised to sample size over the glass transition region for $^{9-10}$FNIII-P in pH 4 buffered solution. The mid-point of the transition ($\Delta C_p = 0.83$ mW) was taken as T'_g (at −70.1 °C). Inset, total heat flow DSC heating thermograms over same region for buffer alone.

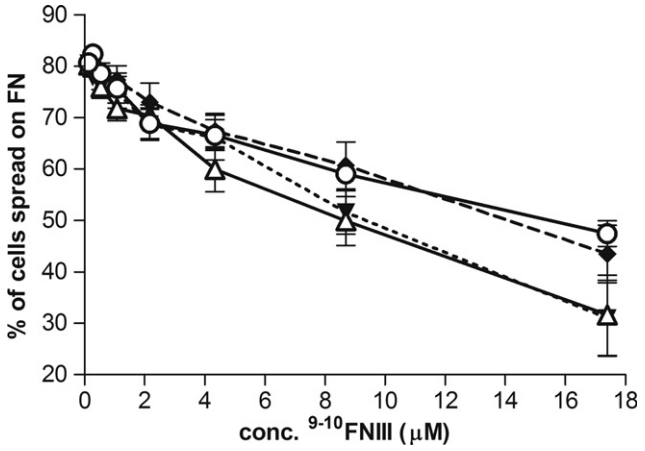

Fig. 9. Inhibition of BHK cell adhesion to FN-coated surfaces by $^{9–10}$FNIII-P, non-lyophilised (○, solid line), lyophilised from pH 4 solution (♦, dashed line), lyophilised with 0.5 M sucrose (▼, dotted line) and with 0.1% PEG 6000 (△, solid line). Adhesion is expressed as the percentage of the respective cell spreading. Error bars represent the sample SEM ($n = 4$).

The functional activity of the lyophilised, reconstituted $^{9–10}$FNIII-P samples was assayed via binding of $^{9–10}$FNIII-P in solution to the cell surface integrin receptors (inhibiting cell adhesion to FN-coated surfaces), as previously described [31]. This assay avoids the effect of possible conformational constraints imposed by the immobilization of $^{9–10}$FNIII-P to a plastic substrate. The positive control used in the assays was non-lyophilised $^{9–10}$FNIII-P, which inhibited cell adhesion to FN surfaces in a dose-dependent manner as previously reported [31]: ca. 80% cell adhesion was observed at $^{9–10}$FNIII-P concentrations <1 μM (normalised to cell adhesion to FN in the absence of $^{9–10}$FNIII-P) falling to ca. 60% cell adhesion at 10 μM (Fig. 9). As for CD analysis of reconstituted protein samples, functional analysis was made for samples lyophilised from pH 4 solution with/without 0.5 M sucrose or 0.1% PEG 6000. By one-way ANOVA the means of the four groups were not statistically different ($P > 0.05$) and no significant difference was found between the lyophilised $^{9–10}$FNIII-P samples versus non-lyophilised $^{9–10}$FNIII-P by Dunnett's post test. Therefore, there appeared to be no benefit in using sucrose or PEG 6000 during the lyophilisation of $^{9–10}$FNIII-P. Consideration of solution formulation conditions for $^{9–10}$FNIII-P would instead appear to mainly depend on a mildly acidic pH. Nevertheless, long term studies investigating the shelf life of solid/liquid formulations of $^{9–10}$FNIII-P would be informative and may further differentiate between the various formulation conditions.

4. Conclusion

Our data demonstrate the importance of using complementary analytical techniques during protein formulation, so that protein unfolding and stability can be related to changes in the secondary structure. $^{9–10}$FNIII-P belongs to the family of β-sandwich proteins and our data show that the addition of PEG or sucrose as excipients does not confer conformational stabilisation. Rather, the addition of sucrose causes a structural intermediate not seen for $^{9–10}$FNIII-P in buffer alone. The ionisation state of the protein appears to be of importance given that it is only at pH 4 that thermal unfolding of $^{9–10}$FNIII-P is (partially) reversible. The best approach to the formulation of the $^{9–10}$FNIII-P is likely to be via simple solution, so avoiding the use of excipients and a lyophilisation cycle.

Acknowledgments

We thank Margaret Nutley, Celine Jones and Jennifer Rouse for scientific and technical support and AstraZeneca for a studentship to PP. The UK Biological Microcalorimetry Facility in Glasgow is funded jointly by the Biotechnology and Biological Sciences Research Council (BBSRC) and Engineering and Physical Sciences Research Council (EPSRC). The Scottish Circular Dichroism Facility is funded by the BBSRC.

References

[1] H.J. Mardon, K.E. Grant, The role of the ninth and tenth type III domains of human fibronectin in cell adhesion, FEBS Lett. 340 (1994) 197–201.
[2] S.M. Cutler, A.J. Garcia, Engineering cell adhesive surfaces that direct integrin alpha5beta1 binding using a recombinant fragment of fibronectin, Biomaterials 24 (2003) 1759–1770.
[3] S. Kim, K. Bell, S.A. Mousa, J.A. Varner, Regulation of angiogenesis in vivo by ligation of integrin alpha5beta1 with the central cell-binding domain of fibronectin, Am. J. Pathol. 156 (2000) 1345–1362.
[4] J.D. Aplin, T. Haigh, C.J. Jones, H.J. Church, L. Vicovac, Development of cytotrophoblast columns from explanted first-trimester human placental villi: role of fibronectin and integrin alpha5beta1, Biol. Reprod. 60 (1999) 828–838.
[5] C.F. van der Walle, H. Altroff, H.J. Mardon, Novel mutant human fibronectin FIII9–10 domain pair with increased conformational stability and biological activity, Protein Eng. 15 (2002) 1021–1024.
[6] B.S. Kendrick, B.S. Chang, T. Arakawa, B. Peterson, T.W. Randolph, M.C. Manning, J.F. Carpenter, Preferential exclusion of sucrose from recombinant interleukin-1 receptor antagonist: role in restricted conformational mobility and compaction of native state, Proc. Natl. Acad. Sci. USA 94 (1997) 11917–11922.
[7] J.C. Lee, S.N. Timasheff, The stabilization of proteins by sucrose, J. Biol. Chem. 256 (1981) 7193–7201.
[8] S.D. Allison, B. Chang, T.W. Randolph, J.F. Carpenter, Hydrogen bonding between sugar and protein is responsible for inhibition of dehydration-induced protein unfolding, Arch. Biochem. Biophys. 365 (1999) 289–298.
[9] W. Wang, Instability, stabilization, and formulation of liquid protein pharmaceuticals, Int. J. Pharm. 185 (1999) 129–188.
[10] A. Cooper, M.W. Kennedy, R.I. Fleming, E.H. Wilson, H. Videler, D.L. Wokosin, T.J. Su, R.J. Green, J.R. Lu, Adsorption of frog foam nest proteins at the air–water interface, Biophys. J. 88 (2005) 2114–2125.
[11] S. Branchu, R.T. Forbes, P. York, H. Nyqvist, A central composite design to investigate the thermal stabilization of lysozyme, Pharm. Res. 16 (1999) 702–708.
[12] M. Cueto, M.J. Dorta, O. Munguia, M. Llabres, New approach to stability assessment of protein solution formulations by differential scanning calorimetry, Int. J. Pharm. 252 (2003) 159–166.

[13] Y. Griko, N. Sreerama, P. Osumi-Davis, R.W. Woody, A.Y. Woody, Thermal and urea-induced unfolding in T7 RNA polymerase: calorimetry, circular dichroism and fluorescence study, Protein Sci. 10 (2001) 845–853.
[14] V. Copie, Y. Tomita, S.K. Akiyama, S. Aota, K.M. Yamada, R.M. Venable, R.W. Pastor, S. Krueger, D.A. Torchia, Solution structure and dynamics of linked cell attachment modules of mouse fibronectin containing the RGD and synergy regions: comparison with the human fibronectin crystal structure, J. Mol. Biol. 277 (1998) 663–682.
[15] D.J. Leahy, I. Aukhil, H.P. Erickson, 2.0 A crystal structure of a four-domain segment of human fibronectin encompassing the RGD loop and synergy region, Cell 84 (1996) 155–164.
[16] E.S. Stevens, E.R. Morris, J.A. Charlton, D.A. Rees, Vacuum ultraviolet circular dichroism of fibronectin. Dominant tyrosine effects, J. Mol. Biol. 197 (1987) 743–745.
[17] M.Y. Khan, G. Villanueva, S.A. Newman, On the origin of the positive band in the far-ultraviolet circular dichroic spectrum of fibronectin, J. Biol. Chem. 264 (1989) 2139–2142.
[18] W. Wang, Lyophilization and development of solid protein pharmaceuticals, Int. J. Pharm. 203 (2000) 1–60.
[19] X.L. Tang, M.J. Pikal, Design of freeze-drying processes for pharmaceuticals: practical advice, Pharm. Res. 21 (2004) 191–200.
[20] J.J. Hill, E.Y. Shalaev, G. Zografi, Thermodynamic and dynamic factors involved in the stability of native protein structure in amorphous solids in relation to levels of hydration, J. Pharm. Sci. 94 (2005) 1636–1667.
[21] L.Q. Chang, D. Shepherd, J. Sun, D. Ouellette, K.L. Grant, X.L. Tang, M.J. Pikal, Mechanism of protein stabilization by sugars during freeze-drying and storage: native structure preservation, specific interaction, and/or immobilization in a glassy matrix? J. Pharm. Sci. 94 (2005) 1427–1444.
[22] W.S. Annan, M. Fairhead, P. Pereira, C.F. van der Walle, Emulsifying performance of modular {beta}-sandwich proteins: the hydrophobic moment and conformational stability, Protein Eng. Des. Sel. 19 (2006) 537–545.
[23] H. Altroff, R. Schlinkert, C.F. van der Walle, A. Bernini, I.D. Campbell, J.M. Werner, H.J. Mardon, Interdomain tilt angle determines integrin-dependent function of the ninth and tenth FIII domains of human fibronectin, J. Biol. Chem. 279 (2004) 55995–56003.
[24] M.D. Pierschbacher, E. Ruoslahti, Cell attachment activity of fibronectin can be duplicated by small synthetic fragments of the molecule, Nature 309 (1984) 30–33.
[25] C. Spitzfaden, R.P. Grant, H.J. Mardon, I.D. Campbell, Module–module interactions in the cell binding region of fibronectin: stability, flexibility and specificity, J. Mol. Biol. 265 (1997) 565–579.
[26] K.W. Plaxco, C. Spitzfaden, I.D. Campbell, C.M. Dobson, A comparison of the folding kinetics and thermodynamics of two homologous fibronectin type III modules, J. Mol. Biol. 270 (1997) 763–770.
[27] B. Farruggia, B. Nerli, H. Di Nuci, R. Rigatusso, G. Pico, Thermal features of the bovine serum albumin unfolding by polyethylene glycols, Int. J. Biol. Macromol. 26 (1999) 23–33.
[28] R. Lumry, H. Eyring, Conformation changes of proteins, J. Phys. Chem. 58 (1954) 110–120.
[29] D. Ringe, G.A. Petsko, The 'glass transition' in protein dynamics: what it is, why it occurs, and how to exploit it, Biophys. Chem. 105 (2003) 667–680.
[30] F. Franks, Solid aqueous-solutions, Pure Appl. Chem. 65 (1993) 2527–2537.
[31] H. Altroff, C.F. van der Walle, J. Asselin, R. Fairless, I.D. Campbell, H.J. Mardon, The eighth FIII domain of human fibronectin promotes integrin alpha5beta1 binding via stabilization of the ninth FIII domain, J. Biol. Chem. 276 (2001) 38885–38892.